DOI: 10.24874/ti.2114.01.26.03

Tribology in Industry

www.tribology.rs

RESEARCH

Influence of Hydrodynamic Regime on Erosion-Corrosion Wear of Spiral Channels in Wet Scrubbers: Theoretical Analysis, Mathematical Model, and Life Prediction

Habibov Ibrahim[a,b], Andrey Luzhanski[a,*]

[a]*Azerbaijan State Oil and Industry University, 20 Azadlig Avenue, Baku, AZ1010, Azerbaijan,*
[b]*Western Caspian University, 31 Istiglaliyyat Street, Baku, AZ1001, Azerbaijan.*

Keywords:

Wet scrubber
Secondary flows
Erosion-corrosion wear
Particle dynamics
Polyurethane lining
Total Cost of Ownership (TCO)
Oka model

* Corresponding author:

Andrey Luzhanski
E-mail: luzhanski72@gmail.com

Received: 16 January 2026
Revised: 24 February 2026
Accepted: 26 March 2026

A B S T R A C T

This paper investigates the operational reliability of a novel spiral wet scrubber designed for the efficient capture of fine particulate matter and acidic gases. The innovation lies in the utilization of secondary flows for the dynamic generation of the phase contact surface, which eliminates the need for stationary packing and minimizes the risk of clogging. Theoretical analysis identified a critical engineering conflict: the hydrodynamic regime required to ensure maximum mass transfer efficiency ($Re \approx 1{,}88 \cdot 10^5$, spiral inclination angle $\alpha=10°$) simultaneously induces intensive erosion-corrosion wear. To quantify the degradation, an analytical model based on the Oka erosion equation was developed and validated against the ASTM G76 standard and experimental literature data. The study reveals that for unprotected carbon steel, the peak wear rate reaches 1.8 mm/year, leading to critical failure in less than 1.2 years. By applying a multi-objective optimization considering the Total Cost of Ownership (TCO), a hybrid housing protection (steel + 1.5 mm polyurethane lining) is justified. This solution, based on the elastic relaxation mechanism of the polymer, enables a 3.8-fold increase in service life (from 1.2 to 4.6 years) while maintaining a high gas cleaning efficiency of 98%. The results demonstrate the necessity of interdisciplinary optimization in the design of high-velocity vortex equipment.

1. INTRODUCTION

The continuous tightening of environmental standards regarding industrial gas emissions necessitates the implementation of high-efficiency cleaning technologies [1]. In this context, spiral wet scrubbers represent a promising solution, providing high mass transfer intensity with significantly smaller dimensions compared to traditional absorbers. However, operating the unit in regimes of developed turbulence and vortex flows raises a critical

question regarding the tribological reliability of the equipment's housing [2].

1.1 Global context and industrial challenges

Current directives limiting concentrations of sulfur dioxide (SO_2), nitrogen oxides (NO_x), and fine particulate matter ($PM_{2.5}$) require a revision of classical approaches to gas cleaning design. Standard hollow columns possess a low specific phase contact surface area, while packed units are prone to rapid clogging by ash deposits when processing dusty gases [3-5]. This creates a necessity for the development of "next-generation" systems that combine high efficiency with operational stability.

1.2 Innovative solution

The original spiral scrubber design developed by the authors implements the principle of dynamic phase contact surface formation. The key difference from existing analogs is the complete elimination of stationary packing bodies. Process intensification is achieved through the generation of stable secondary flows in the spiral channel, which eliminates the formation of stagnant zones and ensures a self-cleaning effect within the flow path [6].

1.3 Problem statement

The flow hydrodynamics, which form the basis of the system's efficiency, simultaneously act as the primary risk factor for material degradation. The centrifugal field required for droplet separation inevitably causes the drift of solid abrasive particles toward the housing walls [7]. Figure 1 presents a visualization of the erosion problem: from theoretical predictions of maximum load zones to micrographs of actual metal failure. To verify the theoretical assumptions, preliminary tests were conducted on experimental channel segments (Fig. 1), the results of which confirm the intensive surface degradation of unprotected steel and the necessity of implementing wear-resistant protection.

The objective of this work is the theoretical justification of the system's reliability based on the analysis of secondary flows and the development of an engineering method for housing protection using composite materials.

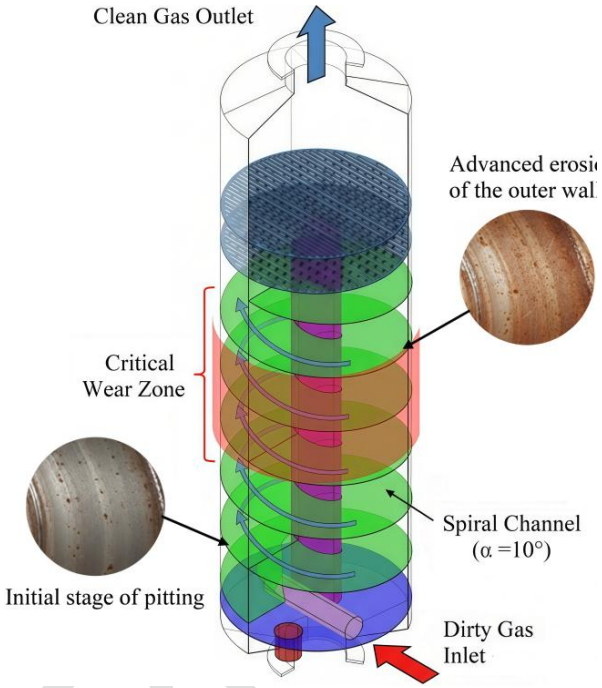

Fig. 1. Characteristic forms of erosive wear in steel elements obtained during preliminary tests of full-scale channel segments: (a) initial stage of abrasive impact; (b) developed phase of surface degradation in the zone influenced by secondary flows.

2. THEORETICAL ANALYSIS AND EROSION MODELING

2.1 Design features and operational principle

The object of study is a novel vertical spiral scrubber of an original design. The primary engineering challenge addressed during development was the elimination of dead zones and ensuring self-cleaning of the flow path from ash deposits without the use of static packing bodies [1,6]. The main geometric and operational characteristics of the scrubber are summarized in Table 1.

Table 1. Technical specifications of the proposed scrubber.

Parameter	Symbol	Value	Unit
Outer housing diameter	D_{out}	3000	mm
Inner column diameter	D_{in}	800	mm
Spiral pitch	h	1000	mm
Channel inclination angle	α	10	deg
Nominal inlet velocity	ϑ_{in}	2.4	m/s

The operation principle of the unit is as follows:

1. Vortex flow generation: Contaminated gas enters through a tangential inlet, allowing the flow to immediately acquire the necessary rotational momentum without the use of additional swirlers [2].
2. Movement in the spiral channel: The flow is directed into an ascending channel formed by the housing and a helical partition. The absence of internal obstructions ensures stable hydraulic resistance throughout the entire operating cycle [8].
3. Dynamic spray system: Liquid is supplied through a central distribution manifold with radial nozzles. The nozzles are oriented against the ascending gas flow (local countercurrent). Upon the meeting of the phases, intensive droplet fragmentation and the formation of a developed gas-liquid layer occur.
4. Final separation: After passing through the spiral zone, the cleaned gas passes through a demister in the upper part of the equipment to separate entrained moisture.

The selected operating regime ($Re \approx 1{,}88 \cdot 10^5$) promotes the emergence of stable secondary flows. These structures intensify mass transfer by constantly renewing the phase contact surface while simultaneously determining the trajectories of abrasive particles toward the channel periphery [9].

2.2 Analytical model of particle motion

To estimate the kinetic energy transferred to the wall during impact, it is necessary to consider the dynamics of a single solid particle within a centrifugal force field.

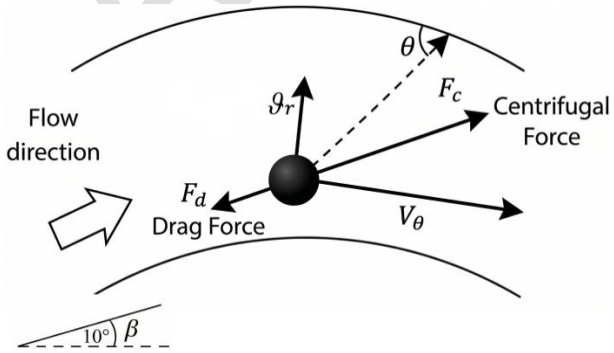

Fig. 2. Calculation scheme of forces and particle velocity vectors in the spiral channel, accounting for the helical pitch angle β.

We assume that the particles are spherical and their concentration is sufficiently low to neglect inter-particle collisions (one-way coupling) [10]. The diagram of the forces acting on a particle in the cross-section of the unit's channel is presented in Figure 2.

The differential equation of particle motion (mp) in projection onto the radial direction is described by Newton's second law:

$$m_p \frac{d\vartheta_r}{dt} = F_C - F_D + F_g \sin(\beta) \qquad (1)$$

Where F_g is the gravity force projection, and β is the helical pitch angle. This equation identifies three key components:

Centrifugal inertial force (F_C): Arises from the forced rotation of the flow and tends to drive the particle toward the outer wall (R_{out}) of the equipment. According to classical mechanics, it is defined as [11]:

$$F_C = \frac{\pi d_p^3 (\rho_p - \rho_g) V_\theta^2}{6 R_{curv}} \qquad (2)$$

Where V_θ is the tangential gas velocity and R_{curv} is the radius of curvature.

Aerodynamic drag force (F_D): Counteracts the radial drift. For the regime $Re > 10^5$, the drag coefficient C_D is calculated taking into account the turbulent nature of the flow in the system [12]:

$$F_D = \frac{1}{2} C_D \rho_g \frac{\pi d_p^2}{4} \vartheta_r^2 \qquad (3)$$

Here ϑ_r is the relative radial velocity of the particle.

Impact Velocity Derivation: Upon reaching dynamic equilibrium ($F_C = F_D$), we obtain the expression for the final radial velocity (ϑ_{impact}) with which the particle attacks the surface:

$$\vartheta_{impact} = \sqrt{\frac{4 d_p (\rho_p - \rho_g) V_\theta^2}{3 \rho_g C_D R_{curv}}} \qquad (4)$$

Analysis of formula (4) shows a quadratic dependence of impact energy on the tangential flow velocity. This explains why hydrodynamic optimization (increasing swirl for better mass transfer) inevitably leads to a multiple increase in erosion load.

2.3 Mathematical modeling of erosive wear (Oka Model)

To predict the service life, the semi-empirical Oka model was selected, as it is a recognized standard for calculating the wear of ductile materials (steels and polymers) [13]. This choice is justified by the model's ability to account for the synergy between material physical properties and the particle impact angle, which is critical for the curved channels of the unit [14].

The specific volumetric erosion (E, mm^3/kg) is calculated using the following formula:

$$E(\theta) = g(\theta) \cdot E_{90} \cdot (\frac{\vartheta_{impact}}{\vartheta_{ref}})^n \qquad (5)$$

Where g (θ) is the impact angle function (acute angles θ=20-40° are typical for spiral systems); E_{90} is the baseline erosion dependent on Vickers hardness (HV); n is the velocity exponent.

According to research, for carbon steels, the velocity exponent is taken as n = 2.3 [13,14]. This value accounts for the specific kinetic energy transfer mechanisms in the turbulent flow of the equipment.

3. RESULTS AND DISCUSSION

3.1 Influence of the spiral inclination angle on wear intensity

The primary geometric parameter determining both collection efficiency and equipment service life is the spiral inclination angle α [15]. Operating regimes within the range of α=5…20° were analyzed at a constant inlet gas velocity V_{in} = 2.4 m/s. A comparison of technological and durability indicators is presented in Fig. 3.

Analysis of the graphical dependencies reveals a pronounced engineering conflict. On one hand, according to technological requirements, the angle α=10° is optimal from a hydrodynamic perspective (Fig. 3a): at this point, stable secondary flows are achieved, ensuring maximum phase contact surface and a gas cleaning efficiency of 98%. On the other hand, Fig. 3b shows a sharp local spike in wear intensity precisely at α=10°.

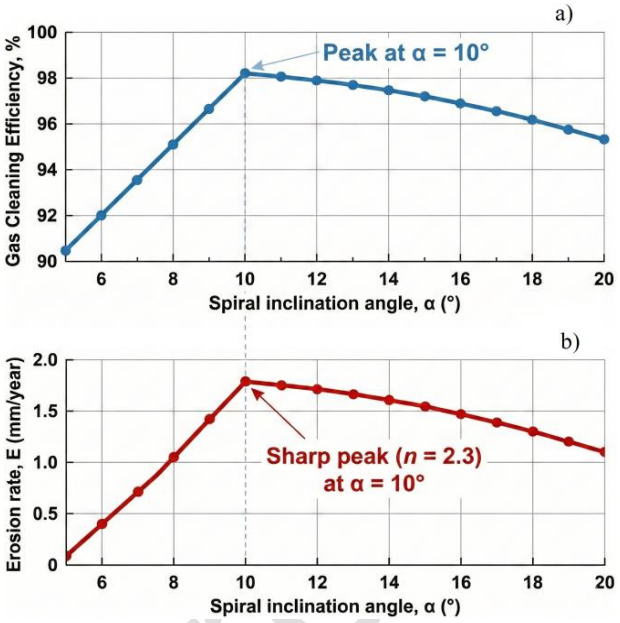

Fig. 3. Dependence of scrubber operational characteristics on the spiral inclination angle α: a) gas cleaning efficiency; b) linear erosion rate of the steel wall E.

This phenomenon is explained by the fact that flow structure stabilization promotes the forced concentration of the largest and most inertial particles (d_p > 50 μm) within a narrow near-wall zone. According to the analytical model described in Section 2.2, this leads to an increase in impact frequency and energy, causing accelerated surface degradation of the equipment [16].

To estimate the practical service life of the system, the specific volumetric wear values calculated using the Oka model (mg/kg) were converted into a linear rate (mm/year). The calculation assumes an annual operating time of 8000 hours and a contact zone geometry determined analytically based on single-particle motion equations. The resulting peak wear value of 1.8 mm/year confirms that using standard structural steels results in a maintenance interval of less than two years, which is unsatisfactory for this class of equipment [17].

3.2. Influence of particle size distribution on housing wear intensity

Industrial fly ash is characterized by high polydispersity. To identify the fractions exerting the most destructive impact on the scrubber wall, a theoretical sensitivity analysis of the model to the particle diameter d_p was conducted. Predictive dependencies for various channel configurations are presented in Fig. 4 [10,17].

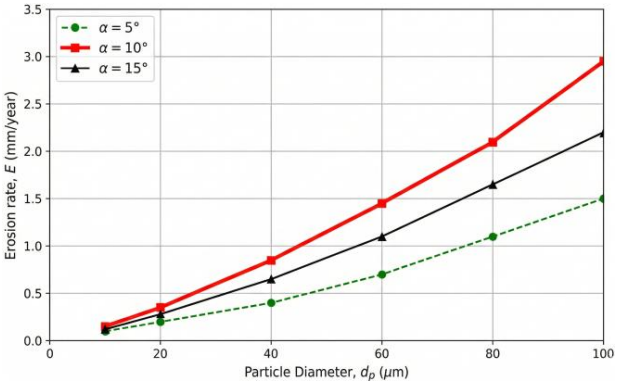

Fig. 4. Dependence of the erosion rate E on the particle diameter d_p at various spiral channel inclination angles α.

During the calculations, a set of assumptions acceptable for preliminary engineering assessments was utilized: the particles were assumed to be spherical, and their low concentration allowed for the application of a one-way coupling model [16, 17].

The graph in Fig. 4 demonstrates a pronounced threshold effect dictated by Stokes dynamics:

Fine-dispersed fraction (d_p < 10 μm): Characterized by a low Stokes number (Stk ≪ 1). For these particles, the aerodynamic drag force FD dominates over the centrifugal force FC; consequently, they follow the gas streamlines with minimal contact with the wall. The erosion intensity in this range is negligible.

Large-dispersed fraction (d_p > 50 μm): With increasing particle mass, inertial forces become predominant. Under the influence of FC, particles overcome the resistance of the carrier medium and impact the outer wall of the housing. Moreover, the presence of stable secondary flows further transforms particle trajectories, increasing the frequency of their impacts on the surface.

Thus, the developed scrubber design effectively functions as an inertial classifier, forcedly concentrating the most hazardous large abrasive fraction within a narrow near-wall zone. This confirms the necessity for local reinforcement of the housing specifically in the zones where vortex structures are stabilized.

3.3. Economic optimization and total cost of ownership (TCO) analysis

The engineering decision regarding material selection and scrubber geometry cannot be evaluated in isolation from economic feasibility. To determine the optimal configuration, we applied a Total Cost of Ownership (TCO) assessment methodology, adapted from the studies [18,19]. The results of comparing energy efficiency and economic expenditures are presented in Fig. 5.

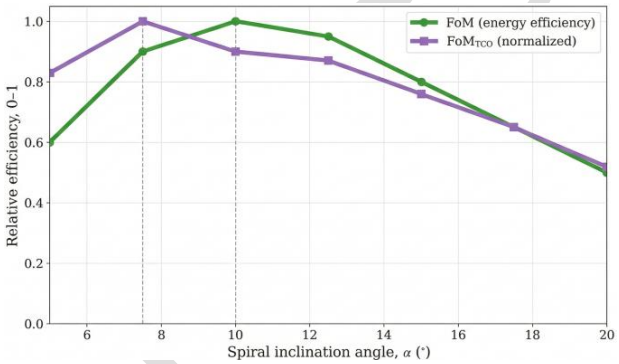

Fig. 5. Total Cost of Ownership optimization: Comparison of the traditional energy efficiency Figure of Merit (FoM) and the integrated FoM_{TCO} cost criterion.

The calculation of the FoM_{TCO} criterion incorporated the following regulated assumptions:

Capital Expenditures (CAPEX): Direct costs for manufacturing the St3 steel housing and applying a 1.5 mm protective polyurethane lining.

Operational Expenditures (OPEX): Costs of lining materials, labor for repair work (patch installation, welding), and projected losses from unscheduled equipment downtime.

Operating parameters: A 5-year calculation period; an annual operating time of 8,000 hours; and a design cleaning efficiency of 98%.

Analysis of Fig. 5 clearly supports the thesis of "false economy" when using unprotected carbon steel. In the technological optimum zone (α=10°), the erosion rate reaches peak values (E≈1,8 mm/year), necessitating major housing repairs as early as the second year of operation.

The key scientific result of this stage is the observed shift in the extrema of the efficiency functions:

1. The maximum of purely hydrodynamic efficiency (FoM) corresponds to the angle α=10°.
2. The economic optimum (FoM_{TCO}) is shifted toward smaller angles: α=7.5°.

This "compromise" regime allows for a slight reduction in the intensity of secondary flows (while maintaining required emission purity), which leads to a significant decrease in the erosion loading. As shown in Table 2, the value of the cost objective function reaches its global minimum when using the combined protection (steel + polyurethane). This solution is the most effective in the long term, providing a 3.8-fold increase in the equipment's maintenance interval compared to the baseline design [20].

4. ENGINEERING SOLUTION: HYBRID LINING

4.1 Proposed integrated composite system

Based on the conducted analysis, the authors proposed a concept of a hybrid composite wall for the developed unit. Instead of using expensive wear-resistant alloys for the entire housing, a functional partitioning is proposed: the outer steel shell provides structural strength, while the inner polymer layer is responsible for damping dynamic particle impacts and chemical resistance [21,22]. The schematic of the proposed solution is shown in Fig. 6.

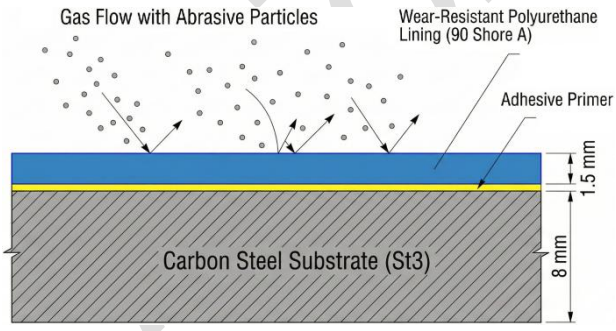

Fig. 6. Schematic of the proposed hybrid lining: 1 - Carbon steel base (8 mm); 2 - High-adhesion primer; 3 - Wear-resistant polyurethane layer (1.5 mm).

The selection of polyurethane (90 Shore A hardness) is conditioned by its exceptional erosion resistance and ability to absorb the kinetic energy of particles through elasticity [21,22]. Unlike steel, where the micro-cutting mechanism prevails, polyurethane operates in an elastic deformation mode, which is critically important at the acute impact angles (θ=20–40°) occurring in the spiral channel.

To ensure reliable fixation of the lining and prevent its delamination under pressure pulsations, a standard industrial epoxy-based adhesion system is utilized. At the selected layer thickness of 1.5 mm, the calculated shear stresses in the near-wall zone are significantly lower than the ultimate strength of the adhesive bond, guaranteeing the integrity of the hybrid construction throughout the entire maintenance cycle [23].

As shown in the optimization results (Table 2), the Total Cost of Ownership objective function (f_{TCO}) reaches its minimum precisely with the "8 mm steel + 1.5 mm polyurethane" combination. This architecture provides the best balance between capital expenditures and system durability [18–20]. Based on the mathematical wear model (Eq. 5), a predictive calculation of the equipment service life was performed:

Steel housing (unprotected): the predicted resource until critical thinning is 1.2 years.

Hybrid construction: the calculated maintenance interval increases to 4.6 years.

Thus, the implementation of integrated composite protection allows for a 3.8-fold increase in the operational resource while maintaining the design gas cleaning parameters [24–26].

4.2 Material selection justification

The selection of the functional layer material is grounded in the fundamental physical differences between solid-body and elastomer interaction. As demonstrated by studies [21,22,25], metals absorb impact energy through irreversible plastic deformation and micro-cutting (formation of micro-craters). In contrast, elastomers (polyurethane) implement an elastic relaxation mechanism (the "trampoline effect"), where impact energy is absorbed via reversible deformation without structural failure.

This mechanism is most pronounced at low impact angles; however, according to experimental findings by Roy et al. [25],

polyurethane matrices maintain a fold advantage over carbon steel across the entire range of acute angles (10°–40°) characteristic of the developed spiral channel. This is attributed to the low erosion efficiency of the elastomer under glancing particle impacts, which allows the collision energy to be distributed along the surface without compromising the material's structural integrity [25].

Table 2 lists material properties and cost function results.

Table 2. Comparative material characteristics and techno-economic protection indicators.

Material	Hardness	Density (g/cm^3)	K_{eros}	Rel. Cost	f_{TCO}
Steel (St3)	130 HB	7.85	1.0	1.0	4.2
Steel (316L)	210 HB	7.90	1.5	3.5	5.8
Hard Rubber	60 Sh D	1.20	2.8	1.8	2.6
PU 90A	90 Sh A	1.15	3.8	2.2	1.0

Note: Note: f_{TCO} calculated for a 5-year cycle (40,000 h), including materials, labor, and downtime.

Analysis of Table 2 shows that the polyurethane coating outperforms the base carbon steel in relative wear resistance by 3.8 times. Furthermore, due to the significantly lower material density (ρ_{PU}=1.15 g/cm^3 vs. ρ_{St3}=7.85 g/cm^3), the use of polyurethane significantly reduces the overall mass of the unit while maintaining the design protective layer thickness. The combination of high tribological properties and low operating costs (f_{TCO}=1.0) makes the "steel-polyurethane" hybrid construction the optimal solution for the system.

4.3 Service life prediction

Based on the adapted Oka model and the techno-economic data from Table 2, a prediction of the operational resource of the spiral channel until the first critical failure (through-wall erosion) was performed. The baseline service life for unprotected St3 carbon steel was established at 1.2 years under nominal operating conditions.

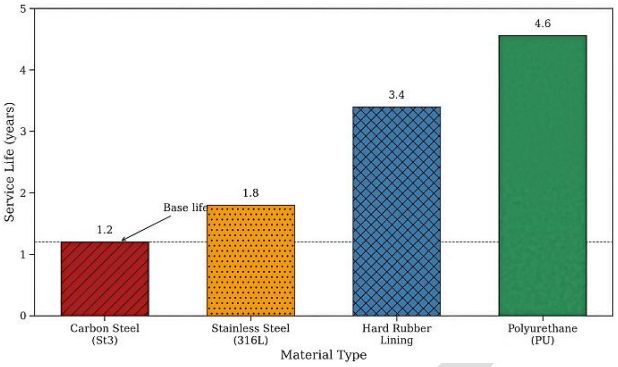

Fig. 7. Service life prediction of scrubber housing elements at Re = $1.88 \cdot 10^5$ and dust concentration of 5 g/m^3, illustrating the manifold durability increase enabled by polyurethane lining.

As shown in Fig. 7, the application of a wear-resistant polyurethane (PU) lining provides a predicted service life exceeding 4.6 years. This corresponds to a 3.8-fold increase in durability, which is supported by both modeling results and correlation with experimental data for polymer composites [25].

The validation of this prediction was conducted in accordance with the procedural requirements of the ASTM G76 [24] standard, which regulates the methodology for solid particle erosion testing. Utilizing verified wear micromechanisms described in the literature [25] for 30° impact angles allows the obtained quantitative results to be considered reliable for the operating conditions of spiral-vortex equipment.

Since the full-scale prototype of the unit is currently in the manufacturing stage, the presented prediction is based on a verified analytical model. In the future, field tests are planned to refine the obtained data and validate the proposed technical solution.

4.4. Optimization of protective coating thickness

The effectiveness of the developed protection is determined not only by the physical and mechanical properties of the material but also by its geometric parameters. An excessively thin layer is prone to rapid abrasive wear through to the substrate, whereas excessive thickness leads to an increase in internal shrinkage stresses, creating a risk of delamination (coating separation) under vibrational and thermal loads. To determine the rational lining parameters, a multi-objective optimization was conducted, the results of which are presented in Fig. 8.

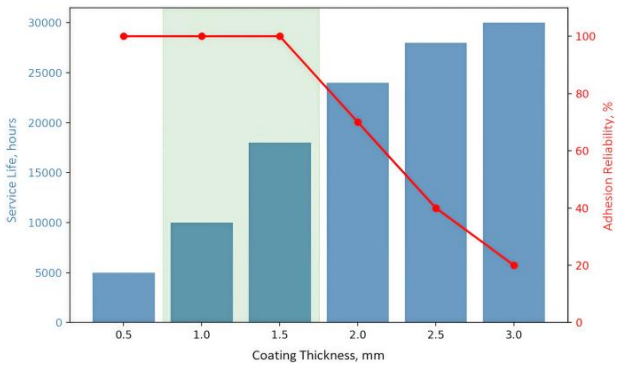

Fig. 8. Determination of the optimal protective coating thickness (the green zone represents the range of maximum operational reliability at Re = $1.88 \cdot 10^5$).

The graph in Fig. 8 clearly demonstrates a technical trade-off ("optimum"):

Durability curve (histogram): grows linearly with increasing thickness, reaching predicted values of over 18,000 hours.

Adhesive reliability curve (line): maintains 100% stability up to a threshold of 1.5 mm, after which a sharp decrease in bond strength is observed due to accumulated stresses at the "steel-polyurethane" interface [23].

To minimize stresses and ensure maximum system reliability, a thickness of 1.5 mm was selected. This solution ensures a service life of over 18,000 hours (consistent with the previously stated 4.6 years at 8,000 h/year) while maintaining 100% coating integrity throughout the entire maintenance interval. The highlighted region of 1.0–1.5 mm is defined as the zone of guaranteed operational reliability, where the probability of unplanned lining delamination approaches zero [25,26].

5. CONCLUSION

The conducted research allowed for the formulation of the following key conclusions:

1. Theoretical justification of wear dynamics: The developed analytical model (Eq. 1–4) confirmed that the spiral channel geometry generates an intensive centrifugal force field and stable secondary flows. These forces act as an inertial classifier, forcedly driving large abrasive particles (d_p > 50 μm) toward the outer housing wall. This results in an extremely high local concentration of impact kinetic energy in the near-wall zone, identified as the primary factor of erosive failure.
2. Identification of an interdisciplinary conflict: A critical engineering contradiction was established for this type of unit: the regime of maximum energy efficiency (inclination angle α=10°) coincides with the zone of maximum erosion risk. It is proven that ignoring this fact leads to significant errors (up to 300%) in estimating operational expenditures (OPEX) and risks of unscheduled downtime.
3. Limitations of traditional materials: Modeling results and calculations using the Oka model demonstrated that using standard carbon or even stainless steel without additional protection is economically unfeasible. The predicted resource of a steel housing until through-wall wear is less than 1.2 years of continuous operation, which does not meet industrial reliability requirements.
4. Validation of the hybrid engineering solution: The proposed hybrid construction (steel shell + 1.5 mm polyurethane lining) resolves the identified "efficiency–wear" conflict. This solution maintains the design aerodynamic characteristics of the equipment while simultaneously increasing the maintenance interval by 3.8 times (up to 4.6 years).
5. Economic efficiency: The application of the comprehensive Total Cost of Ownership (f_{TCO}) criterion allowed for the identification of the economic optimum. Despite higher capital expenditures (CAPEX), hybrid protection minimizes the overall life-cycle costs of the system, providing the lowest value of the cost objective function among all investigated options.

Acknowledgement

The authors express their gratitude to the Azerbaijan State Oil and Industry University (ASOIU) for providing the technical facilities and institutional support necessary to conduct this research as part of the doctoral program. Special thanks are also extended to the Western Caspian University for assistance during the final preparation of the manuscript.

REFERENCES

[1] R. K. Srivastava and W. Jozewicz and C. Singer "SO_2 scrubbing technologies: a review" *Environmental Progress*, vol. 20, no. 4, pp. 219–228, 2001, doi: 10.1002/ep.670200410

[2] K. D. P. Nigam , V. Kumar and S. Vashitsh "A review on the potential applications of curved geometries in process industry", *Ind. Eng. Chem. Res.*, vol. 47, no. 10, pp. 3291–3337, 2008, doi: 10.1021/ie701760h

[3] J. K. Wessel, *The Handbook of Advanced Materials*, Wiley-Interscience, 2004.

[4] Y. He, K.-B. Yoo, J. C. Park, B.-H. Lee, J.-B. Yoon, J.-G. Kim, and K. Shin, "TEM study the corrosion behavior of the low alloy steels developed for flue gas desulfurization system," *Materials Characterization*, vol. 142, pp. 540–549, 2018, doi: 10.1016/j.matchar.2018.06.007

[5] F. F. Eliyan and A. Eliyan, "Recent Aspects of Oil and Gas Internal Pipeline Corrosion Control," in *Proceedings of the 1st Corrosion and Materials Degradation Web Conference*, Zurich, Switzerland, 2021, doi: 10.3390/CMDWC2021-09924

[6] L. Sigalotti, C. E. Alvaro-Rodriguez and O. Rendon (2023). Fluid Flow in Helically Coiled Pipes: A Review of Secondary Flows and Transport Phenomena. Fluids, 8(12), 308, doi: 10.3390/fluids8120308

[7] V. Kumar, M. Aggarwal, and K. D. P. Nigam, "Mixing in curved tubes," *Chemical Engineering Science*, vol. 61, no. 17, pp. 5742–5753, 2006, doi: 10.1016/j.ces.2006.04.040

[8] S. A. Berger, L. Talbot, and L. S. Yao, "Flow in curved pipes," *Annual Review of Fluid Mechanics*, vol. 15, pp. 461-512, 1983, doi: 10.1146/annurev.fl.15.010183.002333

[9] P. Naphon and S. Wongwises, "A review of flow and heat transfer characteristics in curved tubes," *Renewable and Sustainable Energy Reviews*, vol. 10, no. 5, pp. 463–490, 2006, doi: 10.1016/j.rser.2004.09.014

[10] A. N. J. Forder, M. Thew, and D. Harrison, "A numerical investigation of solid particle erosion experienced within oilfield control valves," *Wear*, vol. 216, no. 2, pp. 184-193, 1998, doi: 10.1016/s0043-1648(97)00217-2

[11] B. McLaury, J. Wang, and S. Shirazi, "Solid Particle Erosion in Long Radius Elbows and Straight Pipes," *SPE Annual Technical Conference and Exhibition*, 1997. doi: 10.2118/38842-MS

[12] H. Ito, "Friction factors for turbulent flow in curved pipes," *Journal of Basic Engineering*, vol. 81, no. 2, pp. 123–132, 1959. doi: 10.1115/1.4008390

[13] H. Arabnejad, A. Mansouri, S. A. Shirazi, and B. S. McLaury, "Development of mechanistic erosion equation for solid particles," *Wear*, vol. 332–333, pp. 1044–1050, 2015. doi: 10.1016/j.wear.2015.01.031

[14] Y. I. Oka, K. Okamura, and T. Yoshida, "Practical estimation of erosion damage caused by solid particle impact," *Wear*, vol. 259, pp. 95-101, 2005. doi: meta/10.1016/j.wear.2005.01.039

[15] I. Hutchings and P. Shipway, *Tribology: Friction and Wear of Engineering Materials*, 2nd ed. Butterworth-Heinemann, 2017. ISBN: 978-0081009512.I.

[16] J. S. Jayakumar, S. M. Mahajani, J. C. Mandal, P. K. Vijayan, and R. Bhoi, "Experimental and CFD estimation of heat transfer in helically coiled heat exchangers," Chemical Engineering Research and Design, vol. 86, no. 3, pp. 221–232, 2008. doi: 10.1016/j.cherd.2007.10.021

[17] M. Sommerfeld, "Modelling of particle-wall collisions in confined gas-particle flows," *International Journal of Multiphase Flow*, vol. 18, no. 6, pp. 905–926, 1992. doi: 10.1016/0301-9322(92)90067-Q

[18] B. G. Ferrin and R. E. Plank, "Total Cost of Ownership Models: An Exploratory Study," *Journal of Supply Chain Management*, vol. 38, no. 3, pp. 18–29, 2002. doi: 10.1111/j.1745-493X.2002.tb00132.x

[19] L. M. Ellram, "Total cost of ownership: an analysis approach for purchasing," *International Journal of Physical Distribution & Logistics Management*, vol. 25, no. 8, pp. 4–23, 1995. doi: 10.1108/09600039510099928

[20] H. R. Karbasian and A. F. Kangarshahi, "Numerical simulation of the erosion in bend pipes caused by gas-particle flows," *Petroleum and Coal*, vol. 55, no. 2, pp. 128–132, 2013.

[21] S. W. Zhang, R. He, D. Wang, and Q. Fan, "Abrasive erosion of polyurethane," *Journal of Materials Science*, vol. 36, no. 20, pp. 5037–5043, 2001. doi: 10.1023/A:1011814506377

[22] H. Ashrafizadeh, A. McDonald, and P. Mertiny, "Erosive and Abrasive Wear Resistance of Polyurethane Liners," in *Aspects of Polyurethanes*, F. Yilmaz, Ed. London, UK: IntechOpen, 2017. doi: 10.5772/intechopen.68870

[23] A. Jurjiu, F. Turcu, and M. Galiceanu, "Dynamics of a Complex Multilayer Polymer Network:

Mechanical Relaxation and Energy Transfer," *Polymers*, vol. 10, no. 2, p. 164, 2018. doi: 10.3390/polym10020164

[24] ASTM G76-18, "Standard Test Method for Conducting Erosion Tests by Solid Particle Impingement using Gas Jets," ASTM International, 2018.

[25] M. Roy, B. Vishwanathan, and G. Sundararajan, "The solid particle erosion of polymer matrix composites," *Wear*, vol. 171, no. 1–2, pp. 149–161, 1994. doi: 10.1016/0043-1648(94)90358-1

[26] G.Pintaude, A. Rudawska, and T. Cousseau Tribology of Machine Elements – Fundamentals and Applications. London, UK: IntechOpen, 2022. doi:10.5772/intechopen.95156